ELSEVIER

Computers & Geosciences 30 (2004) 345–353

COMPUTERS & GEOSCIENCES

www.elsevier.com/locate/cageo

Urban 3D GIS From LiDAR and digital aerial images

Guoqing Zhou[a,*], C. Song[a], J. Simmers[b], P. Cheng[c]

[a] *Lab for Earth Observation and Data Processing, Department of Civil Engineering and Technology, Old Dominion University, Kaufmann Hall, Rm. 214, Norfolk, VA 23529, USA*

[b] *Virginia Department of Transportation, 1401 East Broad St., Richmond, VA 23219, USA*

[c] *East China Institute of Technology, Fuzhou, 340000, China*

Received 9 December 2002; accepted 21 August 2003

Abstract

This paper presents a method, which integrates image knowledge and *Li*ght *D*etection *A*nd *R*anging (LiDAR) point cloud data for urban digital terrain model (DTM) and digital building model (DBM) generation. The DBM is an Object-Oriented data structure, in which each building is considered as a building object, i.e., an entity of the building class. The attributes of each building include roof types, polygons of the roof surfaces, height, parameters describing the roof surfaces, and the LiDAR point array within the roof surfaces. Each polygon represents a roof surface of building. This type of data structure is flexible for adding other building attributes in future, such as texture information and wall information. Using image knowledge extracted, we developed a new method of interpolating LiDAR raw data into grid digital surface model (DSM) with considering the steep discontinuities of buildings. In this interpolation method, the LiDAR data points, which are located in the polygon of roof surfaces, first are determined, and then interpolation via planar equation is employed for grid DSM generation. The basic steps of our research are: (1) edge detection by digital image processing algorithms; (2) complete extraction of the building roof edges by digital image processing and human–computer interactive operation; (3) establishment of DBM; (4) generation of DTM by removing surface objects. Finally, we implement the above functions by MS VC++ programming. The outcome of urban 3D DSM, DTM and DBM is exported into urban database for urban 3D GIS.

Keywords: Digital terrain model; Image processing; Digital building model; Interpolation method; 3D GIS

1. Introduction

There is an increasing need for urban three-dimensional (3D) model for various applications such as town planning, microclimate investigation, transmitter placement in telecommunication, noise simulation, heat and exhaust spreading in big cities, virtual city reality, etc. Traditionally, photogrammetry is an important tool to acquire the 3D data. During the past decade, digital photogrammetric methods for providing automatic digital surface model (DSM), or digital terrain model (DTM) generation have become widely used due to the efficiency and cost effectiveness of the production process. The performance of these systems is very good for smooth terrain at small to medium scale when using small and medium scale imagery. However, it decreases rapidly for complex scenes in dense urban areas using large-scale imagery. The degradation in the performance of photogrammetric processes is mainly due to the failures of image matching, which are primarily caused by, for example, occlusions, depth discontinuities, shadows, poor or repeated textures, poor image quality, foreshortening and motion artifacts, and the lack of model of man-made objects (Zhou et al., 1999). To offset the effect of these problems, the extraction of buildings and DTM generation in urban areas are currently still done by human-guided interactive operations, such as stereo compilation from a screen.

*Corresponding author. Tel.: +1-757-683-3619; fax: +1-757-683-5655.

E-mail address: gzhou@odu.edu (G. Zhou).

0098-3004/$ - see front matter © 2004 Elsevier Ltd. All rights reserved.
doi:10.1016/j.cageo.2003.08.012

The whole process is both costly and time-consuming. Over the past years, a lot of researchers in the fields of photogrammetry and computer vision have been striving to develop a comprehensive, high success rate and reliable systems with either full automation or semi-automation to ease human–computer interactive operations. However, automatically extracting building information is still an essentially unsolved problem. A lot of efforts for overcoming the problems mentioned above still are needed.

In the current years, *Li*ght *D*etection *A*nd *R*anging (LiDAR) is widely applied in urban 3D data analysis. A variety of different methods have been proposed for this purpose, some of which can be found from Tao and Hu (2001). Baltsavias et al. (1995) discuss three different approaches for this purpose, namely using an edge operator, mathematical morphology, and height bins for detection of objects higher than the surrounding topographic surface. These main approaches are also used by other authors like Haala (1995), and Eckstein and Munkelt (1995). They analyzed the compactness of height bins, or used mathematical morphology (Eckstein and Munkelt, 1995; Hug, 1997). Hug (1997) applies mathematical morphology in order to obtain an initial segmentation, and the reflectance data are used to discern man-made objects from natural ones via a binary classification. Other building extraction methods include the extraction of plannar patches, some of which use height, slope and/or aspect images for segmentation (e.g., Morgan and Tempfli, 2000; Haala et al., 1998; Morgan and Habib, 2002). In general, these methods can be grouped into two categories (Yoon et al., 2002): classification approach and adjustment approach. The classification approach detects the ground points using certain operators designed based on mathematical morphology (Lindenberger, 1993; Vosselman, 2000) or terrain slope (Axelsson, 1999) or local elevation difference (Wang et al., 2001). Refined classification approach uses Triangulated Irregular Network (TIN) data structure (Axelsson, 2000; Vosselman and Mass, 2001) and iterative calculation (Axelsson, 2000; Sithole, 2001) to consider the discontinuity in the LiDAR data or terrain surface. The adjustment approach essentially uses a mathematical function to approximate the ground surface, which is determined in an iterative least adjustment process while outliers of non-ground points are detected and eliminated (Kraus and Pfeifer, 1998, 2001; Schickler and Thorpe, 2001). Although of efforts have been made in urban 3D data analysis, difficulties still remain. The DTM generation from LiDAR data is not yet mature (Vosselman and Maas, 2001; Yoon et al., 2002). It has been realized, also by many other photogrammetrists, that methods based on single terrain characteristic or criterion can hardly obtain satisfactory results in all terrain types.

In this study, we propose to combine LiDAR data and orthoimage data for urban 3D DBM, DSM and DTM generation. First, the image processing for edge detection is conducted from orthoimages; image interpretation is performed to recognize the building, tree, road, etc., and then to integrate the image knowledge into LiDAR point cloud for the 3D models of DSM, DBM and DTM. Finally, we realize these functions with Microsoft Visual C++. An urban 3D DTM, DBM and DSM are exported to urban database for urban 3D GIS.

2. Building detection and extraction

2.1. Edge detection from orthoimage

As described above, the building extraction based on either images or LiDAR data cannot reach a satisfactory result. One of main causes is because of breaklines for urban building. It is thus very important to extract the breaklines of building before applying any interpolation technique because the breaklines can be used to identify the sudden change in slope or elevation. Therefore, detecting breaklines will serve both interpolation and building extraction. In urban areas most of the breaklines represent parts of artificial objects such as building. In digital image, a breakline (edge) is a sharp discontinuity in gray-level profile. Thus, simplest edge detection method is to inspect the change of the digital number of each pixel in a neighboring region with the first derivative or the second derivative of the brightness. A lot of edge detection methods have been developed in the past decades in image processing community. However, the situation is complicated by the presence of noise, image resolution, object complexity, occlusion, shadow, etc. Our implementation of building edge detection is that the zero-cross edge detection operator is first employed, and then some post-processing, such as merging line segment into line, deleting isolated point and line segment is carried out. Finally, an human–computer interactive operation is employed for extraction of complete edges of objects. These extracted edges of objects, associated with the planimetric coordinates are coded and saved in files in vector format for the interpretation and interpolation of objects (see the description in Section 2.2).

2.2. Image interpretation and building extraction

After the complete edges of buildings have been detected, the algorithms for extraction of the building geometrical parameters for interpretation of objects will be performed. The LiDAR data interpretation is based on the two facts: (1) The buildings are higher than the surrounding topographic surface; (2) The ability of the laser to penetrate vegetation, thus giving echo from several heights, makes it possible to distinguish between the two classes: man-made objects and vegetation. The

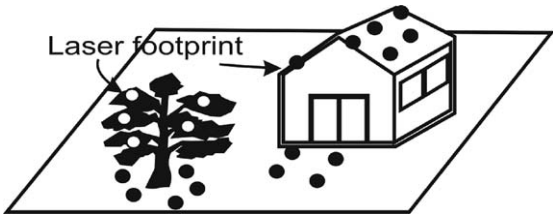

Fig. 1. LiDAR footprints on building and vegetation.

extraction procedures are based on an implementation of the minimum description length (MDL) criterion for robust estimation (Rissanen, 1983; Axelsson, 1992). Thus, main steps are (1) linking the 2D complete image edges of building with 3D LiDAR data using horizontal coordinates, (2) determining the three-dimensional building breaklines from image edges and exactly estimating the building boundary via integrating image edges and LiDAR, and (3) interpreting the LiDAR data for buildings or vegetation using two facts and MDL. Internal breaklines can be determined by intersecting the adjacent planar facades within the building. It is known that the laser points are not selective, and they do not match building boundary. Therefore, one cannot determine the building boundary with only height data unless the density of LiDAR point cloud is like image gray representation. Fig. 1 shows a portion of a building near its boundary. Some laser data points are located on the building, while others are located on the ground. The segments of LiDAR data therefore is from the image segments, which describe various building. Therefore, we have selected the geo-referenced images whose 2D geodetic coordinates are known. We can directly use the planimetric coordinates of the boundary edges to obtain each 3D building model. The building boundary in addition to the internal façade parameters and the internal 3D breaklines will be the results of the building extraction process. The topological relationships of building facades is described in Section 3.

3. Digitally modeling buildings

In our research, an object-oriented data structure has been developed for the description of digital building model (DBM). During the development of this model, we mainly think of making best use of the data sets for better creating DBM for buildings, for instance the roof, which we have obtained from the geo-referenced image providing the information of roof, and the LiDAR data, which provide information of the height of building. In this model, each building is an object of the building class, i.e., an entity of the class. One building object consists of the attributes of the Building ID, roof type ID, and the series of the roof surfaces. Each surface in the surface series of a building object is also considered an object. The surface's class is comprised of the surface's boundary, the LiDAR footprints within the surface and planar equation parameters describing the surface by fitting LiDAR footprints. The boundary is composed of a set of points. One of advantages of this model is its flexibility for future expanding, e.g., adding other building attributes, such as wall surfaces, texture, etc. (see Fig. 2). We implement this data structure as follows:

```
typedef struct{   double dx;
          double dy;
          double dElevation;
} LiDARPoint;
class CBuilding : public CObject
{
protected:   unsigned m_nBID; // Building ID
          unsigned m_nRoofType; //Roof Type
       ID
public:   CTypedPtrList<CObList,
       CSurface* > m_surfaceList;
       //Surfaces series in one building
……
……
……
};
class CSurface : public Cobject
{
public:   //Planar equation parameters
          double m_dP1;
          double m_dP2;
          double m_dP3;
public:   CArray<CPoint,          CPoint>
       m_ptEdgeArray;
          //Point array on behalf of the surface
       boundary
             CArray<LiDARPoint,    LiDAR-
       Point> m_ptLiDARArrayIn;
          //Series of LiDAR points within the
       footprint of the surface
       ……
       ……
       ……
       };
```

4. Creation of digital surface model (DSM)

4.1. Establishment of the relationship between images and LiDAR point cloud data

The orthoimages are stored as raster data, while the LiDAR point cloud is collected along track. The linkage

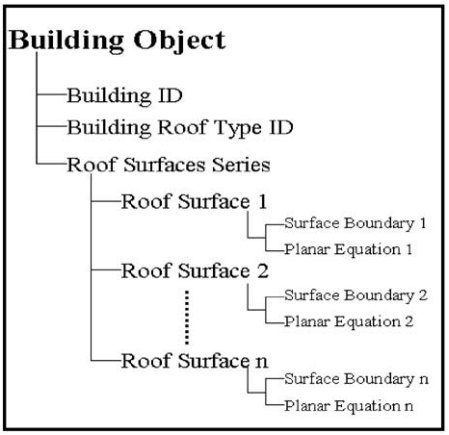

Fig. 2. Object-oriented DBM.

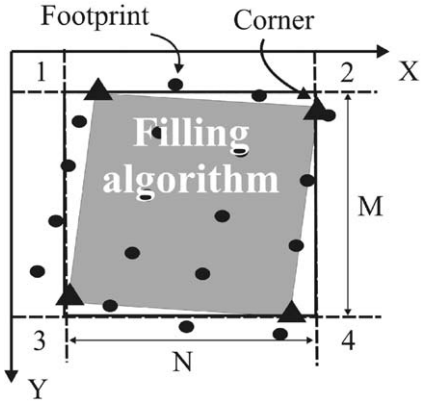

Fig. 3. Determination of inside footpoints in building using filling algorithm.

of the two data sets is implemented by the planimetric coordinates. Thus, we have to determine which LiDAR footprints are inside of boundary of a building. We use filling algorithm, whose steps are (note that a rectangle is selected as a sample in Fig. 3):

- *Create polygon of roof's surface:* The edge of a roof surface that we extracted from the orthoimage is a set of point coordinates like $(x_1, y_1; x_2, y_2; \ldots; x_n, y_n)$. We can obtain the surface polygon by connecting the edge points orderly in this step.
- *Obtain the boundary of the polygon of the roof surface:* For a given roof surface, for example, the coordinates of 4 corner points of its boundary rectangular can be obtained by (see Fig. 3):

Corner 1: $(X_1,\ Y_1)$
Corner 2: $(X_2,\ Y_2)$
Corner 3: $(X_3,\ Y_3)$
Corner 4: $(X_4,\ Y_4)$

- *Obtain the reduced LiDAR points within the boundary rectangular:* For speeding up the calculation, we reduce the LiDAR points via the test to see whether these points are in the roof surface or not. By simple comparison of the LiDAR point coordinates and the rectangular corners, we can obtain the reduced LiDAR points.
- *Determine the LiDAR footpoints in the reduced points:* The determination of the LiDAR footprints in the reduced points are inside or outside is carried out by filling algorithm. This algorithm was realized by Microsoft MFC function, i.e., CRgn::PtInRegion in MS VC++.

This procedure is then repeated for roof plane of each building until all buildings are implemented.

4.2. Interpolation algorithm via planar equation

After we obtained a complete extraction of the roof surfaces, we will be able to obtain the LiDAR points within the footprint of the roof surfaces and store them into an array in a surface object of a building, whose procedure was described in Section 4.1. Now, each building object has its LiDAR point data, associated with boundary information. We use the information to generate the DSM of urban areas. There are many interpolation methods available. However, these methods cannot meet the accuracy requirement, such as Inverse Distance Weight (IDW) method, which calculate the unknown elevation by using the close known neighbors, and give them different weight on the basis of the distance between them and the unknown points. We here suggest an innovative method for LiDAR data interpolation. The basic principle is to fit the roof surfaces of building using planar equation. The equation is solved by the LiDAR footprints within roof boundary that we already obtained in Section 4.1. The planar equation is

$$AX + BY + CZ = 1, \tag{1}$$

where A, B, and C are unknown parameters, and X, Y and Z are coordinates of LiDAR data. At least three LiDAR footprints are requested to determine the planar equation (surface of building). However, usually, more than three footprints are measured in each surface. Least-squares method is thus employed to calculate the parameters of the planar equation. The equation is

$$\begin{bmatrix} X_1, Y_1, Z_1 \\ X_2, Y_2, Z_2 \\ \cdots \\ X_m, Y_m, Z_m \end{bmatrix} \times \begin{Bmatrix} A \\ B \\ C \end{Bmatrix} = \begin{Bmatrix} 1 \\ 1 \\ \cdots \\ 1 \end{Bmatrix}, \tag{2}$$

where m is the number of LiDAR points in a surface.

This interpolation method for DSM generation via planar equation and the surface boundary can reach higher accuracy than the method via LiDAR raw data array interpolation within the boundary.

5. Creation of digital terrain model (DTM)

LiDAR data presents two aspects: ground and buildings. Thus, the data could be segmented into two types of regions corresponding, on one hand, to a surface linked to the ground, and, on the other hand, to a surface linked to surface objects. Therefore, DTM can be generated by separation of the surface objects from the DSM. The DBM has been generated above, and the DTM can be generated by removing the surface objects. The steps are:

(1) Based on the extracted boundary of building in image processing, we can get the planimetric coordinates of these boundary points.
(2) Seeking for corresponding LiDAR footprints according to planimetric coordinates.
(3) Removing those LiDAR footprints whose planimetric coordinates are same the one of building boundary.
(4) Interpolating the DTM via the IDW method.

6. Experiments

6.1. Data sets

The Virginia Department of Transportation (VDOT), contracting to Woolpert LLC at Richmond, Virginia, has established a high-accuracy test field in Wytheville, Virginia. It consists of approximately 21 targeted ground points placed specifically for airborne LiDAR data collection and accuracy test purposes. The field extends from the west side of Wytheville east approximately 114 miles, with a north–south extent of approximately 4.5 miles centered on Wytheville, i.e., from latitude, 36°54′16″ to 36°59′54″ North, and from longitude, 81°08′23″ to 81°49′08″ West (see Fig. 4). The target points are spaced at least several kilometers apart and distributed in a generally east–west direction (see Fig. 4). The point accuracy can attain standard deviations better than 0.02, 0.02, and 0.10 m in X, Y and Z, respectively. This level of accuracy is comparable with geodetic accuracy standard for Order C (1.0 cm plus 10 ppm). This control field will be used for our test of orientation parameter determination.

6.1.1. Lidar data

The LiDAR data were obtained by using an Optech 1210 LiDAR system in September 2000. The LiDAR data have accuracy (on hard surfaces) of 2.0-feet at least and point sampling density is sufficient to provide an average post spacing of 7.3-feet in the raw DSM. It was provided in raw text format. The LiDAR parameters used for this project are as follows:

- Aircraft speed: 202 ft/s
- Flying height: 4500 ft above ground level
- Scanner field of view (half angle): $\pm 16^\circ$
- Scan frequency: 14 Hz
- Swath width: 2581 ft (1806 ft with a 30% sidelap)
- Pulse repetition rate: 10 kHz
- Sampling density: average 7.3 ft

6.1.2. Aerial image data

To aid planimetric compilation, quality control of the LiDAR data, the analog black-and-white aerial

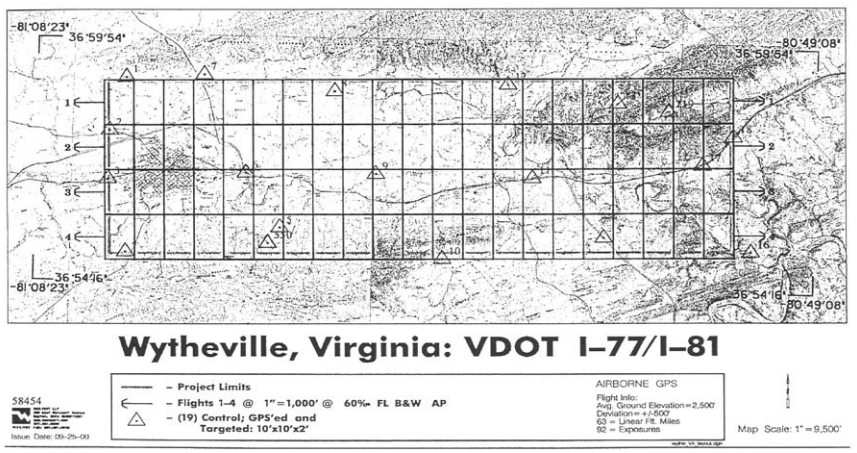

Fig. 4. Geodetic control test field in Wytheville, VA.

photography was acquired along east–west flight lines over the project area on September 19, 2000 at a scale of 1:1000. Woolpert camera number 5099 was used. Kodak 2405 file was used with a 525-nm filter and 153.087 mm focal length. A total of 96 exposures were acquired over 4 equal length flight lines (see Fig. 4). Aerial photo has a pixel resolution of 2.0-feet, and the orthoimage was produced using fully differential rectification techniques and the LiDAR DTM. All the elevation data were referenced to NAVD88 datum; and horizontal data were referenced to NAD83/93 Virginia State Plane Coordinate system. The city of Wytheville, Virginia, lies in the west part of the data coverage. As the availability of data and its precision, we selected the data of southern part of the city for our study (Fig. 5).

6.2. System development

We developed a system of semi-automation urban 3D model generation from LiDAR data and image data using Microsoft Visual C++ platform. The system consists of the following modules (Fig. 6):

(1) *New/open a project:* This module opens an existing or create new project.
(2) *LiDAR data check:* This module is to check the systematic error of LiDAR data via various methods, such as overlay LiDAR data onto georeferenced image, ground control points checks, etc.
(3) *Data input (image and LiDAR):* This module contains LiDAR data input, image display, data format conversion (e.g., for raw image to bmp image, tiff image format, etc.) (see Fig. 7).
(4) *Image processing and interactive edit:* This module contains image filtering, enhancement, edge detection, line feature and area detection and description, image interpretation, interactive operation, etc.
(5) *Topology generation of building and DBM:* This module is to implement the functions of topologic description of building and of DBM using object-oriented data structure.
(6) *Urban DSM and DTM generation:* This module is to generate high-accuracy of DSM by applying the surface equation; some conventional interpolation methods, such as IDW, are available. The DTM is generated by removing surface objects.

By this software, a group of experimental results are listed in Figs. 8–13, Fig. 8 is the result of automatic detection of building edge, and Fig. 9 depicts the detected buildings after human–computer interactive

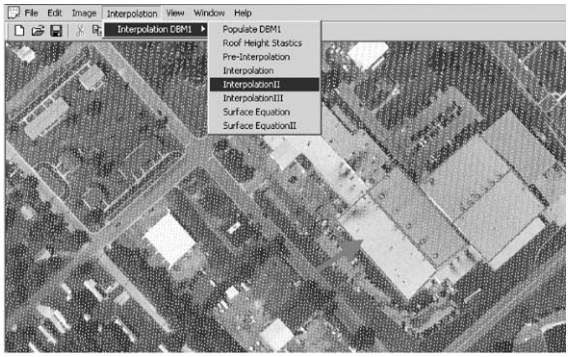

Fig. 6. Semi-automatic urban 3D model generation system, in which dot points are LiDAR point cloud; and lines are extracted edges of buildings.

Fig. 7. Patch of original image.

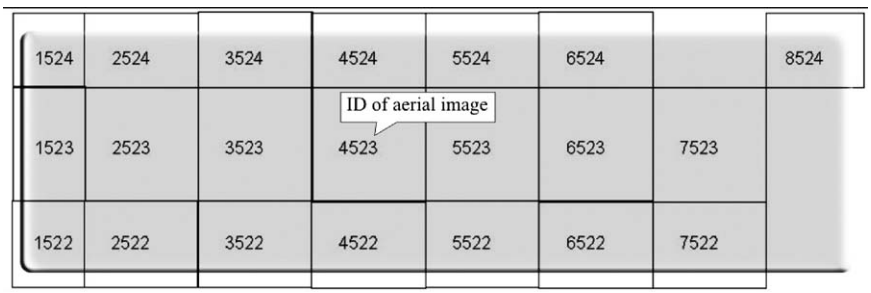

Fig. 5. Configuration for aerial image and LiDAR data collection (shadowed areas indicate coverage of LiDAR data, and number indicates ID of aerial images).

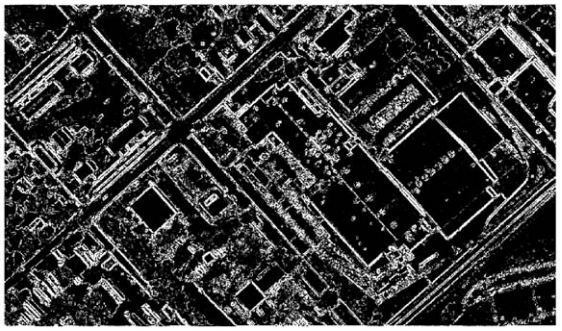

Fig. 8. Automatically detected building edges.

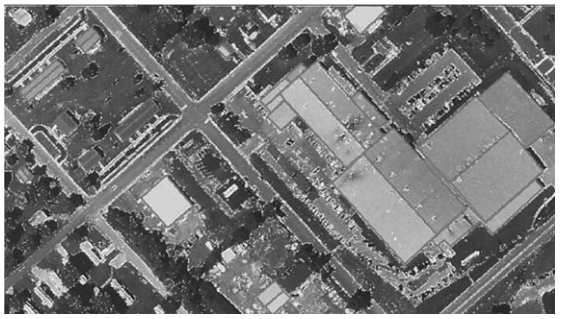

Fig. 9. Detected building edges by human–computer interaction operation.

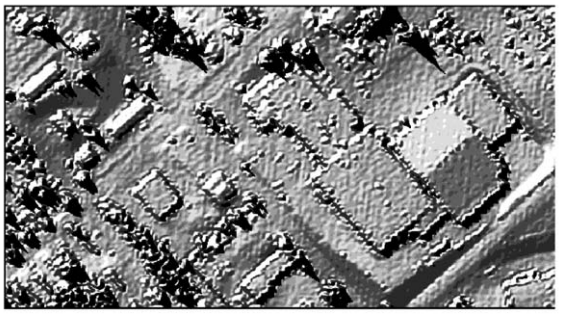

Fig. 10. Result of raw LiDAR data interpolated by IDW.

operation. Fig. 12 depicts the DSM, which is generated by our algorithm. In order to compare the interpolation accuracy between our method and other interpolation methods, e.g., the IDW method and Spline method, the results from IDW and Spline methods are shown in Figs. 10 and 11. As we can see, the two interpretation methods cannot reach high accuracy. The building edges are not very clear. It appears that there are dim slopes to the ground. Also, the roof surfaces are rough, but the most of real roof surfaces are planar. Obviously, our

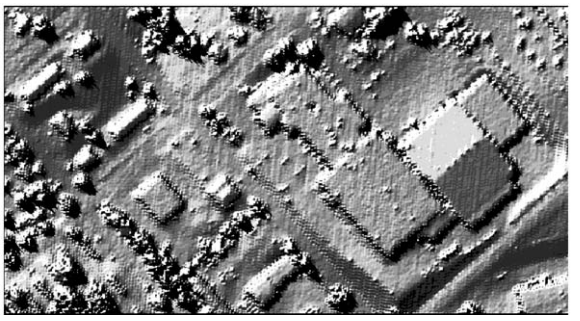

Fig. 11. Result of raw LiDAR data interpolated by Spline (Spline parameters are: weight = 0.1, number of points = 12, type is regularized).

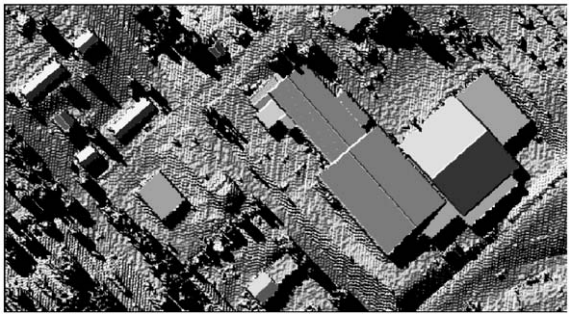

Fig. 12. Result of raw LiDAR data interpolated by our software.

interpolation result is much better than IDW and Spline methods. The edges and the roof surfaces are clearer. Fig. 13 is DBM.

7. Conclusion

In this paper, we presented the generation of urban 3D model, including 3D DSM, DBM and DTM via integrating image knowledge and LiDAR. A human–computer interactive operation system has been developed for this purpose. The main contributions of this paper are to develop a high-accuracy interpolation method for DBM/DTM/DSM generation and to develop an object-oriented building model. In this model, we defined the roof types, roof surfaces, planar equation parameters, etc. Especially, the model consisted of roof surface's boundary and their planar equations, which are from the combined processing of the LiDAR data and orthoimage data. For planar equation of each roof surface, we firstly extract the LiDAR point data lying within it by their spatial relationship, and then calculate the planar equation's parameters with these LiDAR points by least-square method. We use the planar equation to calculate the gird value within the roofs.

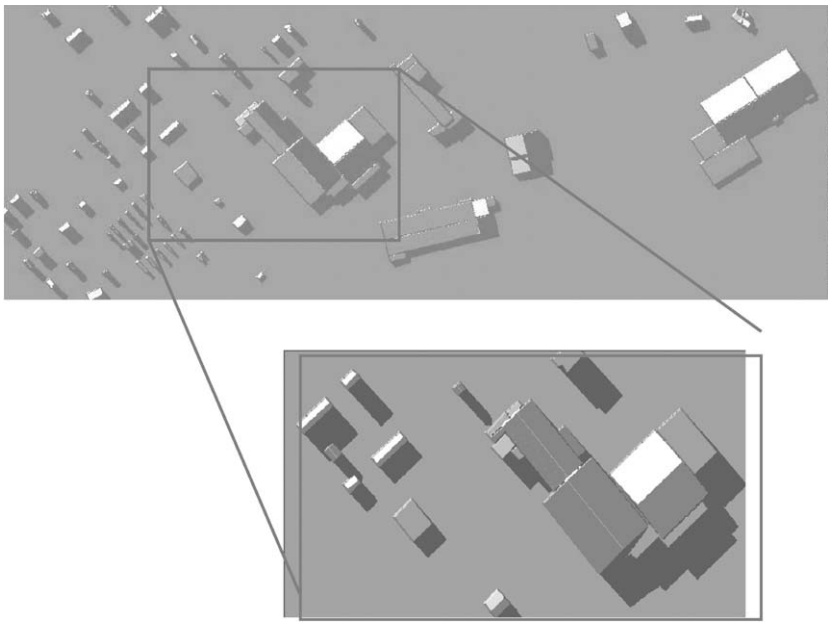

Fig. 13. Urban DBM generated by our software system.

The experiment demonstrated that the high accuracy of DSM, DBM and DTM in urban areas has been reached via our software system.

Acknowledgements

The project is financially supported by US National Science Foundation (NSF) under contract number NSF 0131893. The experimental data were provided by the Virginia Department of Transportation and Woolpert LLC at Richmond, Virginia. We especially thank Frank Sokoloski and Qian Xiao very much for our discussion in the technology of LiDAR data processing and development of system as well as for their kind helps in LiDAR data check and delivery.

References

Axelsson, P., 1992. Minimum description length as an estimator with robust properties. In: Foerstner, W., Ruwiedel, S. (Eds.), Robust Computer Vision. Wichmann, Eerlag, Karlsruhe, pp. 137–150.

Axelsson, P., 1999. Processing of laser scanner data-algorithms and applications. ISPRS Journal of Photogrammetry and Remote Sensing, Vol. 54, pp. 138–147.

Axelsson, P., 2000. DEM generation from laser scanner data using adaptive TIN models. International Archive of Photogrammetry and Remote Sensing XXXIII (Part B4), pp. 110–117.

Baltsavias, E., et al., 1995. Use of DTMs/DSMs and orthoimages to support building extraction. In: Gruen, A., Kubler, O.A.P. (Eds.), Automatic Extraction of Man-Mad Objects from Aerial and Space Images. Birkhaeuser, Basel, pp. 199–210.

Eckstein, W., Munkelt, O., 1995. Extracting objects from digital terrain models. In: Schenk, T. (Ed.), Remote Sensing and Reconstruction for Three-Dimensional Objects and Scenes. Proceedings of SPIE Symposium on Optical Science, Engineering, and Instrumentation, Vol. 2572, San Diego.

Haala, N., 1995. 3D building reconstruction using linear edge segments. In: Fitsch, D., Hobbie, D. (Eds.), Photogrammetric Week. Wichmann, Karlsruhe, pp. 19–28.

Haala, N., Brenner, C., Anders, K., 1998. Three dimensional urban GIS from laser altimeter and 2D map data. International Archives of Photogrammetry and Remote Sensing 32 (3/1), pp. 339–346.

Hug, C., 1997. Extracting artificial objects from airborne laser scanner data. In: Gruen, A., Baltsavias, E., Henricsson, O. (Eds.), Automatic Extraction of Man-Made Objects from Aerial and Space Images (II). Birkhaeuser, Basel, pp. 203–212.

Kraus, K., Pfeifer, N., 1998. Determination of terrain models in wooded areas with airborne laser scanner data. ISPRS Journal of Photogrammetry and Remote Sensing, Vol. 53, pp. 193–203.

Kraus, K., Pefifer, N., 2001. Advanced DEM generation from LiDAR data. In: Hofton, M.A. (Ed.), Proceedings of the ISPRS Workshop on Land Surface Mapping and Characterization using Laser Altimetry, Annapolis, Maryland. International Archives of the Photogrammetry, Remote

Sensing and Spatial Information Sciences, Vol. XXXIV part 3/W4 Commission III.

Lindenberger, J., 1993. Laser-Profilmessungen zur topographischen Gelaedeaufnahme. Deutsche Geodaetische Kommission, Series C, No. 400, Munich.

Morgan, M., Habib, A., 2002. Interpolation of LiDAR data and automatic building extraction. ASPRS Annual Conference, CD-ROM, Washington, DC, April 19–25.

Morgan, M., Tempfli, K., 2000. Automatic building extraction from airborne laser scanning data. International Archives of Photogrammetry and Remote Sensing 33 (B3), pp. 616–623.

Rissanen, J., 1983. A universal prior for integers and estimation by minimum description length. The Annals of Statistics 11 (2), pp. 416–431.

Schickler, W., Thorpe, A., 2001. Surface estimation based on LiDAR. CD-ROM Proceedings of ASPRS Annual Conference, April 23–27, St. Louis, Missouri, USA.

Sithole, G., 2001. Filtering of laser altimetry data using a slope adaptive filter. In: Hofton, M.A. (Ed.), Proceedings of the ISPRS Workshop on Land Surface Mapping and Characterization Using Laser Altimetry, Annapolis, Maryland. The International Archives of the Photogrammetry, Remote Sensing and Spatial Information Sciences, Vol. XXXIV part 3/W4 Commission III, pp. 203–210.

Tao, C., Hu, Y., 2001. A review of post-processing algorithms for airborne LiDAR data. CD-ROM Proceedings of ASPRS Annual Conference, April 23–27, St. Louis, Missouri, USA.

Vosselman, G., 2000. Slope based filtering of laser altimetry data. International Archives of Photogrammetry and Remote Sensing XXXIII (Part B3), pp. 935–942.

Vosselman, G., Mass, H., 2001. Adjustment and filtering of raw laser altimetry data. Proceedings of the OEEPE Workshop on Airborne Laser scanning and Interferometric SAR for Detailed Digital Elevation Models, Stockholm, 1–3 March.

Wang, Y., Mercer, B., Tao, C., Sharma, J., Crawford, S., 2001. Automatic generation of bald earth digital elevation models from digital surface models created using airborne IFSAR. CD-ROM Proceedings of ASPRS Conference, April 23–27, St. Louis, Missouri, USA.

Yoon, Jong-suk, Shan, J., 2002. Urban DEM generation from raw airborne LiDAR data. ASPRS Annual Conference, CD-ROM, Washington, DC, April 19–25.

Zhou, G., Albertz, J., Gwinner, K., 1999. Extracting 3D information using temporal–spatial analysis of aerial image sequences, Photogrammetry Engineering & Remote Sensing, vol. 65, no. 7, pp. 823–832.